

Rotating polarizer, compensator, and analyzer ellipsometry

Sofyan A. Taya[†], Taher M. El-Agez, and Anas A. Alkanoo

Physics Department, Islamic University of Gaza, Gaza, Palestinian Territories

(Received 9 April 2013; revised manuscript received 21 May 2013)

In this paper we propose theoretically a set of ellipsometric configurations using a rotating polarizer, compensator, and analyzer at a speed ratio of $N_1\omega:N_2\omega:N_3\omega$. Different ellipsometric configurations can be obtained by giving different integral values to N_1 , N_2 , and N_3 . All configurations are applied to bulk c-Si and GaAs to calculate the real and imaginary parts of the refractive index of the samples. The accuracies of all ellipsometric configurations are investigated in the presence of a hypothetical noise and with small misalignments of the optical elements. Moreover, the uncertainties in the ellipsometric parameters as functions of the uncertainties of the Fourier coefficients are studied. The comparison among different configurations reveals that the rotating compensator-analyzer configuration corresponds to the minimum error in the calculated optical parameters.

Keywords: ellipsometry, polarizer, analyzer, compensator

PACS: 07.60.Fs

DOI: 10.1088/1674-1056/22/12/120703

1. Introduction

Ellipsometry has become a standard technique for analyzing bulk materials, thin films, surfaces, and interfaces.^[1-11] In ellipsometry, information about a sample is obtained by measuring and analyzing the change in polarization state when light is reflected at non-normal incidence from a specular surface or transmitted through a sample.^[12] Ellipsometry generally consists of a source, a detector, and polarization-state-conditioning elements such as polarizers and compensators. An ellipsometric measurement allows one to quantify the phase difference between E_p and E_s , Δ , and the ratio of their amplitudes given by $\tan(\psi)$. For a reflecting surface, the forms of Δ and ψ are

$$\Delta = \delta_p - \delta_s, \quad (1)$$

$$\tan \psi = \frac{|r_p|}{|r_s|}, \quad (2)$$

where δ_p and δ_s are the phase changes for the p and s components of light; r_p and r_s are the complex Fresnel reflection coefficients for the p and s components which may be written as

$$\begin{cases} r_p = \rho_p e^{i\delta_p}, \\ r_s = \rho_s e^{i\delta_s}. \end{cases} \quad (3)$$

Ellipsometry allows for the determination of the complex reflectance ratio ρ of a surface. This quantity is defined as the ratio between reflection coefficients of p and s , r_p and r_s . Commonly, the reflectance ratio is expressed in terms of ψ and Δ as

$$\rho = \frac{r_p}{r_s} = \tan(\psi) e^{i\Delta}. \quad (4)$$

The real and imaginary parts of the refractive index can be calculated using the following equations:

$$\varepsilon_r = \sin^2 \theta_0 + \sin^2 \theta_0 \tan^2 \theta_0 \left(\frac{1-\rho}{1+\rho} \right)^2, \quad (5)$$

where θ_0 is the angle of incidence and

$$\begin{aligned} \varepsilon_r &= \varepsilon_1 + i\varepsilon_2, \quad \tilde{n} = \sqrt{\varepsilon} = n + ik, \\ \varepsilon_1 &= n^2 - k^2, \quad \text{and} \quad \varepsilon_2 = 2nk, \end{aligned} \quad (6)$$

where \tilde{n} is the complex refractive index, ε is the permittivity, n is the real part of the refractive index, and k is the imaginary part of the refractive index which is called the extinction factor.

The history of ellipsometry began in 1887 when Drude derived the equations of ellipsometry.^[13] Since then, ellipsometry has attracted researchers and scientists. Until the early 1970s, ellipsometry measurements were time consuming. In 1975, the automation of spectroscopic ellipsometry (SE) measurement was achieved by Aspnes and Studna.^[14] This breakthrough in the field improved the measurement time as well as the measurement precision. In 1984, real time monitoring ellipsometry was constructed.^[15] Since then, different ellipsometric configurations have been studied in the literature.^[16-23] The speed ratio with which the optical elements rotate was the main difference among these structures. The most common configuration was the rotating analyzer ellipsometer.^[16] The rotating polarizer and analyzer ellipsometer (RPAE) has also been proposed in different forms. The most common one was an RPAE with a speed ratio of 1:2.^[17,18] An RPAE in which the polarizer and the analyzer rotate with the ratio 1:1,^[19,20] an RPAE with a speed ratio 1:3,^[21,22] and an RPAE with a speed ratio 1:-1^[23] were among those proposed.

In a recent study, an ellipsometer using a phase retarder and rotating polarizer and analyzer at a speed ratio 1: N was proposed.^[24] Different ellipsometric configurations were presented by assuming $N = 1, 2$, and 3.

[†]Corresponding author. E-mail: staya@iugaza.edu.ps

As recent examples of the applications of SE, the authors in Ref. [25] fabricated the gallium phosphide (GaP) nanoparticulate thin films by colloidal suspension deposition and investigated these films by SE. They used the effective medium approximation to calculate the values of the refractive index n and the extinction coefficient k .

The authors in Ref. [26] analyzed the effect of a spherical shape on the measurement results of SE, and a method to eliminate this effect was proposed. Based on the simulation results of the SE measurement on a silicon sphere by ray tracking, they found that the sphere makes the parallel incident beam of the SE divergent after reflection, and the measurement error of the SE, caused by this phenomenon, can be explained by the mixed polarization theory.

In this work, we propose theoretically a general ellipsometric structure in which three elements are rotating. The speed ratio at which the polarizer, compensator, and analyzer rotate is $N_1\omega:N_2\omega:N_3\omega$, respectively. The approach has the advantage that the equations of any ellipsometric configuration can be obtained just by substituting for N_1, N_2 , and N_3 . We give six examples by assigning N_1, N_2 , and N_3 some specific values and hence six different ellipsometric configurations are studied and compared.

2. Mueller formalism

Stokes vector and Mueller matrix formalisms are usually used to express the theory of ellipsometry. The Stokes vector consists of four elements: S_0, S_1, S_2 , and S_3 . Another approach may be used in the theory of ellipsometry which is Jones vector and Jones matrix formalism. The Jones vector is usually adopted for describing polarized light. In order to describe unpolarized or partially polarized light, the Stokes vector is usually used. In actual ellipsometry measurement, Stokes parameters can be measured. In the Stokes vector representation, optical elements are described by the Mueller matrices.

$$B_m = \begin{bmatrix} 1 & -\cos(2\psi) & 0 & 0 \\ -\cos(2\psi) & 1 & 0 & 0 \\ 0 & 0 & \sin(2\psi)\cos(\Delta) & \sin(2\psi)\sin(\Delta) \\ 0 & 0 & -\sin(2\psi)\sin(\Delta) & \sin(2\psi)\cos(\Delta) \end{bmatrix}. \quad (11)$$

We respectively assume a rotating polarizer, rotating compensator, and rotating analyzer to have angles $\beta_p = N_1P + \gamma$, $\beta_c = N_2P + \kappa$, and $\beta_A = N_3P + \alpha$, where $P = \omega t$, and γ, κ , and α are the initial azimuth angles of the optical elements at $t = 0$. The Stokes vector of the detected light is given by

$$S = R(-\beta_A)A_mR(\beta_A)B_m R(-\beta_c)C_mR(\beta_c) R(-\beta_p)P_mR(\beta_p)P_m S_i, \quad (12)$$

where S is a four-element column vector containing Stokes parameters S_0 through S_3 , and $S_i = [1, 0, 0, 0]^T$.

3. Rotating polarizer, compensator, and analyzer ellipsometer at any speed ratio

After performing the product of matrices given by Eq. (12) and rearranging the result, the detected light intensity

The ellipsometric configurations under consideration consist of light source, fixed linear polarizer, rotating linear polarizer with angular speed $N_1\omega$, rotating compensator with angular speed $N_2\omega$, sample, rotating analyzer with angular speed $N_3\omega$, and detector. The compensator generates a phase difference between the two components of light, given by

$$\delta = \frac{2\pi d}{\lambda}(n_e - n_o), \quad (7)$$

where d is the thickness of the compensator and n_e and n_o are the extraordinary and ordinary refractive indices at the wavelength λ . It is worth mentioning that in experiment, compared with the polarizer and analyzer elements, the compensator is less optically perfect with the retardation angle which is not a constant and usually changes slightly with wavelength in the entire spectral region. The error caused by this part of dispersive features will slightly affect data accuracy of the system.

As the incident light travels through these optical elements, the state of polarization changes. The Mueller matrices associated with the optical elements employed in the proposed ellipsometric structure^[13] are given below.

The matrix of rotation with an angle α , $R(\alpha)$ reads

$$R(\alpha) = \begin{bmatrix} 1 & 0 & 0 & 0 \\ 0 & \cos(2\alpha) & \sin(2\alpha) & 0 \\ 0 & -\sin(2\alpha) & \cos(2\alpha) & 0 \\ 0 & 0 & 0 & 1 \end{bmatrix}, \quad (8)$$

the matrix of an ideal fixed polarizer or analyzer P_m or A_m is

$$P_m = A_m = \frac{1}{2} \begin{bmatrix} 1 & 1 & 0 & 0 \\ 1 & 1 & 0 & 0 \\ 0 & 0 & 0 & 0 \\ 0 & 0 & 0 & 0 \end{bmatrix}, \quad (9)$$

the matrix of an ideal fixed compensator C_m is

$$C_m = \begin{bmatrix} 1 & 0 & 0 & 0 \\ 0 & 1 & 0 & 0 \\ 0 & 0 & \cos(\delta) & \sin(\delta) \\ 0 & 0 & -\sin(\delta) & \cos(\delta) \end{bmatrix}, \quad (10)$$

and the matrix of an ideal sample B_m is

can be found from the first component of the column vector $S(S_0)$. To simplify the result, we let

$$A = 1 - \frac{\cos(2\psi)}{4} - \frac{\cos(2\psi)\cos(\delta)}{4}, \quad (13)$$

$$B = 1 - \frac{\cos(2\psi)}{2} - \frac{\cos(2\psi)\cos(\delta)}{2}, \quad (14)$$

$$C = -\frac{\cos(2\psi)}{4} - \frac{\cos(2\psi)\cos(\delta)}{4}, \quad (15)$$

$$D = -\frac{\cos(2\psi)}{2} + \frac{\cos(2\psi)\cos(\delta)}{2}, \quad (16)$$

$$E = \frac{1}{4} - \cos(2\psi) + \frac{\cos(\delta)}{4}, \quad (17)$$

$$F = \frac{1}{4} - \frac{\cos(2\psi)}{2} + \frac{\cos(\delta)}{4}, \quad (18)$$

$$G = \frac{\sin(2\psi)\cos(\Delta)}{8} + \frac{\sin(2\psi)\cos(\Delta)\cos(\delta)}{8}, \quad (19)$$

$$H = \frac{1}{8} + \frac{\cos(\delta)}{8}, \quad (20)$$

$$J = \frac{1}{8} - \frac{\cos(\delta)}{8}, \quad (21)$$

$$K = \frac{\sin(2\psi)\cos(\Delta)}{4} - \frac{\sin(2\psi)\cos(\Delta)\cos(\delta)}{4}, \quad (22)$$

and

$$L = \frac{-\sin(2\psi)\sin(\Delta)\sin(\delta)}{4}. \quad (23)$$

In terms of these coefficients, the general equation of the detected light intensity can be written as

$$\begin{aligned} I = & A + B \cos(2N_1)P + C \cos(4N_1)P + 2D \cos(4N_2)P \\ & + E \cos(2N_3)P + D \cos 2(2N_2 - N_1)P \\ & + 2D \cos 4(N_2 - N_1)P \\ & + F [\cos 2(N_1 - N_3)P + \cos 2(N_1 + N_3)P] \\ & + 2G [\cos 2(N_1 - N_3)P + \cos 2(N_1 + N_3)P] \\ & + H [\cos 2(2N_1 + N_3)P + \cos 2(2N_1 - N_3)P] \\ & + G [\cos 2(2N_1 + N_3)P - \cos 2(2N_1 - N_3)P] \\ & + J [\cos 2(2N_2 + N_3)P + \cos 2(2N_2 - N_3)P] \\ & + K [\cos 2(2N_2 - N_3)P - \cos 2(2N_2 + N_3)P] \\ & + 2J [\cos 2(2N_2 - N_1 + N_3)P + \cos 2(2N_2 - N_1 - N_3)P] \\ & + 2K [\cos 2(2N_2 - N_1 + N_3)P - \cos 2(2N_2 - N_1 - N_3)P] \\ & + J [\cos 2(2N_1 - 2N_2 + N_3)P + \cos 2(2N_1 - 2N_2 - N_3)P] \\ & + K [\cos 2(2N_1 - 2N_2 + N_3)P - \cos 2(2N_1 - 2N_2 - N_3)P] \\ & + 2L [\cos 2(N_1 - N_2 - N_3)P - \cos 2(N_1 - N_2 + N_3)P] \\ & + L [\cos 2(N_2 + N_3)P - \cos 2(N_2 - N_3)P] \\ & + L [+ \cos 2(2N_1 - N_2 - N_3)P \\ & - \cos 2(2N_1 - N_2 + N_3)P]. \end{aligned} \quad (24)$$

Equation (24) gives a general expression for the intensity received by the detector of the proposed structure. We will consider two cases. In the first case, both the compensator and the analyzer are rotating whereas the polarizer is fixed. In the second case, we will assume that the compensator and the polarizer are rotating whereas the analyzer is fixed. In each case, three ellipsometric configurations are investigated by considering different speed ratios of the rotating elements. Section 4 covers the first case and Section 5 presents the second one.

4. Rotating compensator analyzer ellipsometer with a fixed polarizer

In this case, N_1 is set to be zero while N_2 and N_3 could be any integer. In the following subsections, we assume $\gamma = 0$, $N_2 = 1$, and $N_3 = 1, 2$ or 3 . Three different ellipsometric configurations are then obtained. For each configuration we use the Fourier transform of the intensity to deduce the Fourier coefficients and the ellipsometric parameters.

4.1. Rotating compensator analyzer ellipsometer with a speed ratio 1:1

In the first configuration, the following parameters are assumed to be $N_1 = 0$, $\gamma = 0$, $\kappa = 0$, $\alpha = 0$, and $N_2 = N_3 = 1$. Substituting these values into Eq. (24) and taking the Fourier transform of the result, we have

$$I(t) = a_0 + \sum_{n=1}^3 a_n \cos(2n\omega t), \quad (25)$$

where a_0 and a_n are the Fourier coefficients which are given by

$$\begin{aligned} a_0 = & 2 - \cos(2\psi) - \cos(2\psi)\cos(\delta) \\ & + \sin(2\psi)\sin(\Delta)\sin(\delta), \end{aligned} \quad (26)$$

$$\begin{aligned} a_1 = & \frac{3}{2} - 2\cos(2\psi) + \frac{\cos(\delta)}{2} - \frac{\sin(2\psi)\cos(\Delta)}{2} \\ & - \frac{\sin(2\psi)\cos(\Delta)\cos(\delta)}{2}, \end{aligned} \quad (27)$$

$$\begin{aligned} a_2 = & -\cos(2\psi) + \cos(2\psi)\cos(\delta) \\ & - \sin(2\psi)\sin(\Delta)\sin(\delta), \end{aligned} \quad (28)$$

$$\begin{aligned} a_3 = & \frac{1}{2} - \frac{\cos(\delta)}{2} - \frac{\sin(2\psi)\cos(\Delta)}{2} \\ & + \frac{\sin(2\psi)\cos(\Delta)\cos(\delta)}{2}. \end{aligned} \quad (29)$$

Note that the intensity contains three alternating coefficients (ACs) Fourier coefficients a_1 , a_2 , and a_3 in addition to direct coefficients (DCs) term a_0 . The intensity is symmetric since $\sin(2n\omega t)$ terms are missing, i.e. the intensity has cosine terms only. Solving Eqs. (27)–(29) for $(\tan \psi)$ and $(\cos \Delta)$ we obtain

$$\sin(\psi) = \sqrt{\frac{a_1 + a_3}{4}}, \quad (30)$$

$$\cos(\psi) = \sqrt{\frac{4 - a_1 - a_3}{4}}, \quad (31)$$

$$\tan(\psi) = \sqrt{\frac{a_1 + a_3}{4 - a_1 - a_3}}, \quad (32)$$

and

$$\cos(\Delta) = \frac{-2a_3 + 1 - \cos(\delta)}{2(1 - \cos(\delta))\sin(\psi)\cos(\psi)}. \quad (33)$$

It is worth investigating the uncertainties $\delta\psi$ and $\delta\cos(\Delta)$ in the ellipsometric parameters ψ and Δ due to the fluctuations in the Fourier coefficients. The uncertainties $\delta\psi$ and $\delta\cos(\Delta)$ are calculated by differentiating Eqs. (30) and (31) as follows:

$$\delta\psi = \frac{\delta\psi}{\delta a_1} \delta a_1 + \frac{\delta\psi}{\delta a_3} \delta a_3, \quad (34)$$

$$\delta \cos(\Delta) = \frac{\delta \cos(\Delta)}{\delta a_1} \delta a_1 + \frac{\delta \cos(\Delta)}{\delta a_3} \delta a_3, \quad (35)$$

where

$$\frac{\delta \psi}{\delta a_1} = \frac{1}{1 + \tan^2(\psi)} \frac{1}{8 \cos^2(\psi)} (\cot(\psi) + \tan(\psi)), \quad (36)$$

$$\frac{\delta \psi}{\delta a_3} = \frac{1}{1 + \tan^2(\psi)} \frac{1}{8 \cos^2(\psi)} (\cot(\psi) + \tan(\psi)), \quad (37)$$

$$\frac{\delta \cos(\Delta)}{\delta a_1} = \frac{\cos(\Delta)}{8} \left(\frac{\tan(\psi) - \cot(\psi)}{\sin(\psi) \cos(\psi)} \right), \quad (38)$$

and

$$\frac{\delta \cos(\Delta)}{\delta a_3} = \frac{\cos(\Delta)}{8} \left(\frac{\tan(\psi) - \cot(\psi)}{\sin(\psi) \cos(\psi)} \right) - \frac{1}{(1 - \cos(\delta)) \sin(\psi) \cos(\psi)}. \quad (39)$$

4.2. Rotating compensator analyzer ellipsometer with a speed ratio 1:2

In the second configuration, we assume the following values $\gamma = 0$, $\kappa = 0$, $\alpha = 0$, $N_1 = 0$, $N_2 = 1$, and $N_3 = 2$. The Fourier transformation of Eq. (24) contains one DC and four AC coefficients. It is given by

$$I(t) = a_0 + \sum_{n=1}^4 a_n \cos(2n\omega t), \quad (40)$$

where

$$a_0 = \frac{5}{2} - \frac{\cos(\delta)}{2} - \cos(2\psi) - \cos(2\psi) \cos(\delta) + \sin(2\psi) \cos(\Delta) - \sin(2\psi) \cos(\Delta) \cos(\delta), \quad (41)$$

$$a_1 = \sin(2\psi) \sin(\Delta) \sin(\delta), \quad (42)$$

$$a_2 = 1 - 3 \cos(2\psi) + \cos(2\psi) \cos(\delta), \quad (43)$$

$$a_3 = -\sin(2\psi) \sin(\Delta) \sin(\delta), \quad (44)$$

and

$$a_4 = \frac{1}{2} - \frac{\cos(\delta)}{2} - \frac{\sin(2\psi) \cos(\Delta)}{2} + \frac{\sin(2\psi) \cos(\Delta) \cos(\delta)}{2}. \quad (45)$$

From these Fourier coefficients we can derive ψ and Δ to obtain

$$\tan(\psi) = \sqrt{\frac{-a_2 - 2 + 2 \cos(\delta)}{a_2 - 4}}, \quad (46)$$

$$\cos(\Delta) = \frac{-2a_4 + 1 - \cos(\delta)}{D}, \quad (47)$$

where

$$D = (1 - \cos(\delta)) \sqrt{\frac{a_1^2}{1 - \cos^2(\delta)} + \left(\frac{2a_4 - 1 + \cos(\delta)}{1 - \cos(\delta)} \right)^2}. \quad (48)$$

We differentiate Eqs. (46) and (47) to obtain $\delta \psi$ and $\delta \cos(\Delta)$ as follows:

$$\delta \psi = \frac{\delta \psi}{\delta a_2} \delta a_2, \quad (49)$$

$$\delta \cos(\Delta) = \frac{\delta \cos(\Delta)}{\delta a_1} \delta a_1 + \frac{\delta \cos(\Delta)}{\delta a_4} \delta a_4, \quad (50)$$

where

$$\frac{\delta \psi}{\delta a_2} = \frac{1}{1 + \tan^2(\psi)} \frac{1}{\tan(\psi)} \left(\frac{3 - \cos(\delta)}{(a_2 - 4)^2} \right), \quad (51)$$

$$\frac{\delta \cos(\Delta)}{\delta a_4} = \frac{-2}{D} - \frac{2(2a_4 - 1 + \cos(\delta)) \cos(\Delta)}{D^2}, \quad (52)$$

and

$$\frac{\delta \cos(\Delta)}{\delta a_1} = \frac{\cos(\Delta)}{D^2} \left(\frac{1 - \cos(\delta)}{1 + \cos(\delta)} \right) a_1. \quad (53)$$

4.3. Rotating compensator analyzer ellipsometer with a speed ratio 1:3

Another ellipsometric configuration can be obtained by letting $N_2 = 1$ and $N_3 = 3$ provided that $N_1 = \gamma = 0$, $\kappa = 0$, and $\alpha = 0$. When these values are inserted into Eq. (24), the Fourier transformation is found to have five AC terms in addition to the DC term. It is given by

$$I(t) = a_0 + \sum_{n=1}^5 a_n \cos(2n\omega t), \quad (54)$$

where

$$a_0 = 2 - \cos(2\psi) - \cos(2\psi) \cos(\delta), \quad (55)$$

$$a_1 = \frac{1}{2} - \frac{\cos(\delta)}{2} + \frac{\sin(2\psi) \cos(\Delta)}{2} - \frac{\sin(2\psi) \cos(\Delta) \cos(\delta)}{2}, \quad (56)$$

$$a_2 = \cos(2\psi) + \cos(2\psi) \cos(\delta) + \sin(2\psi) \sin(\Delta) \sin(\delta), \quad (57)$$

$$a_3 = 1 + \cos(\delta) - 2 \cos(2\psi), \quad (58)$$

$$a_4 = -\sin(2\psi) \sin(\Delta) \sin(\delta), \quad (59)$$

and

$$a_5 = \frac{1}{2} - \frac{\cos(\delta)}{2} - \frac{\sin(2\psi) \cos(\Delta)}{2} + \frac{\sin(2\psi) \cos(\Delta) \cos(\delta)}{2}. \quad (60)$$

The ellipsometric parameters ψ and Δ can be derived from these coefficients and we obtain

$$\sin(\psi) = \sqrt{\frac{a_1 + a_3 + a_5}{4}}, \quad (61)$$

$$\cos(\psi) = \sqrt{\frac{3 + \cos(\delta)}{1 - \cos(\delta)} \left(\frac{a_1 + a_5}{4} \right) - \frac{a_3}{4}}, \quad (62)$$

$$\tan(\psi) = \frac{\sin(\psi)}{\cos(\psi)}, \quad (63)$$

$$\cos(\Delta) = \frac{a_1 - a_5}{2(1 - \cos(\delta)) \sin(\psi) \cos(\psi)}. \quad (64)$$

Moreover, the uncertainties of ψ and Δ are given by,

$$\delta \psi = \frac{\delta \psi}{\delta a_1} \delta a_1 + \frac{\delta \psi}{\delta a_3} \delta a_3 + \frac{\delta \psi}{\delta a_5} \delta a_5, \quad (65)$$

$$\delta \cos(\Delta) = \frac{\delta \cos(\Delta)}{\delta a_1} \delta a_1 + \frac{\delta \cos(\Delta)}{\delta a_3} \delta a_3 + \frac{\delta \cos(\Delta)}{\delta a_5} \delta a_5, \quad (66)$$

where

$$\frac{\delta\psi}{\delta a_1} = \frac{1}{1+\tan^2(\psi)} \frac{1}{8\cos^2(\psi)} \times \left(\cot(\psi) - \frac{3+\cos(\delta)}{1-\cos(\delta)} \tan(\psi) \right), \quad (67)$$

$$\frac{\delta\psi}{\delta a_3} = \frac{1}{1+\tan^2(\psi)} \frac{1}{8\cos^2(\psi)} (\cot(\psi) - \tan(\psi)), \quad (68)$$

$$\frac{\delta\psi}{\delta a_5} = \frac{1}{1+\tan^2(\psi)} \frac{1}{8\cos^2(\psi)} \times \left(\cot(\psi) - \frac{3+\cos(\delta)}{1-\cos(\delta)} \tan(\psi) \right), \quad (69)$$

$$\frac{\delta \cos(\Delta)}{\delta a_1} = \frac{1}{E_1} \frac{[(3+\cos(\delta))\tan(\psi) + (1-\cos(\delta))\cot(\psi)]\cos(\Delta)}{4E_1}, \quad (70)$$

$$\frac{\delta \cos(\Delta)}{\delta a_3} = \frac{(1-\cos(\delta))[-\tan(\psi) + \cot(\psi)]\cos(\Delta)}{4E_1}, \quad (71)$$

$$\frac{\delta \cos(\Delta)}{\delta a_5} = \frac{-1}{E_1} \frac{[(3+\cos(\delta))\tan(\psi) + (1-\cos(\delta))\cot(\psi)]\cos(\Delta)}{4E_1}, \quad (72)$$

and

$$E_1 = 2(1-\cos(\delta))\sin(\psi)\cos(\psi). \quad (73)$$

5. Rotating polarizer compensator ellipsometer with a fixed analyzer

We now turn our attention to the second case in which the analyzer is fixed while both the compensator and polarizer are rotating with different ratios. To achieve this, we set $N_3 = 0$ and $\alpha = \pi/4$ while N_1 and N_2 may take any integral values to obtain different ellipsometric configurations as will be shown in the following subsections.

5.1. Rotating polarizer compensator ellipsometer with a speed ratio 1:1

In the first configuration, we assume $N_1 = N_2 = 1$, $\kappa = 0$, and $\gamma = 0$. Substituting these values into Eq. (24) and taking the Fourier transform of the results, we obtain the following expression for the intensity

$$I(t) = a_0 + \sum_{n=1}^2 a_n \cos(2n\omega t) + \sum_{n=1}^2 b_n \sin(2n\omega t), \quad (74)$$

where,

$$a_0 = 1 - \frac{\cos(2\psi)}{2}, \quad (75)$$

$$a_1 = 1 - \cos(2\psi), \quad (76)$$

$$a_2 = \frac{-\cos(2\psi)}{2}, \quad (77)$$

$$b_1 = \sin(2\psi)\cos(\Delta), \quad (78)$$

$$b_2 = \frac{\sin(2\psi)\cos(\Delta)}{2}. \quad (79)$$

For this ellipsometric configuration, ψ and Δ are given in terms of Fourier coefficients as

$$\sin(\psi) = \sqrt{\frac{a_1}{2}}, \quad (80)$$

$$\cos(\psi) = \sqrt{\frac{a_1 - 4a_2}{2}}, \quad (81)$$

$$\tan(\psi) = \sqrt{\frac{a_1}{a_1 - 4a_2}}, \quad (82)$$

$$\cos(\Delta) = \frac{b_1}{2\sin(\psi)\cos(\psi)}. \quad (83)$$

We differentiate the last two equations to obtain $\delta\psi$ and $\delta\cos(\Delta)$ as follows:

$$\delta\psi = \frac{\delta\psi}{\delta a_1}\delta a_1 + \frac{\delta\psi}{\delta a_2}\delta a_2, \quad (84)$$

$$\delta\cos(\Delta) = \frac{\delta\cos(\Delta)}{\delta a_1}\delta a_1 + \frac{\delta\cos(\Delta)}{\delta a_2}\delta a_2 + \frac{\delta\cos(\Delta)}{\delta b_1}\delta b_1, \quad (85)$$

where

$$\frac{\delta\psi}{\delta a_1} = \frac{1}{1+\tan^2(\psi)} \frac{1}{4\cos^2(\psi)} (\cot(\psi) - \tan(\psi)), \quad (86)$$

$$\frac{\delta\psi}{\delta a_2} = \frac{1}{1+\tan^2(\psi)} \frac{1}{4\cos^2(\psi)} (\tan(\psi)), \quad (87)$$

$$\frac{\delta\cos(\Delta)}{\delta a_1} = \frac{-\cos(\Delta)}{4} \left(\frac{1}{\cos^2(\psi)\sin^2(\psi)} \right), \quad (88)$$

$$\frac{\delta\cos(\Delta)}{\delta a_2} = \frac{\cos(\Delta)}{4} \left(\frac{1}{\cos^2(\psi)} \right), \quad (89)$$

and

$$\frac{\delta\cos(\Delta)}{\delta b_1} = \frac{1}{2\sin(\psi)\cos(\psi)}. \quad (90)$$

5.2. Rotating polarizer compensator ellipsometer with a speed ratio 1:2

In the second configuration, we assume the following values: $N_1 = 1$, $N_2 = 2$, $\kappa = 0$, $\gamma = 0$, and $\alpha = \pi/4$. The Fourier transformation of Eq. (24) contains one DC and eight AC coefficients. It is given by

$$I(t) = a_0 + \sum_{n=1}^4 a_n \cos(2n\omega t) + \sum_{n=1}^4 b_n \sin(2n\omega t), \quad (91)$$

where

$$a_0 = 1 - \frac{\cos(2\psi)}{4} - \frac{\cos(2\psi)\cos(\delta)}{4}, \quad (92)$$

$$a_1 = 1 - \frac{\cos(2\psi)}{2} - \frac{\cos(2\psi)\cos(\delta)}{2}, \quad (93)$$

$$a_2 = \frac{-\cos(2\psi)}{2}, \quad (94)$$

$$a_3 = -\frac{\cos(2\psi)}{2} + \frac{\cos(2\psi)\cos(\delta)}{2}, \quad (95)$$

$$a_4 = -\frac{\cos(2\psi)}{4} + \frac{\cos(2\psi)\cos(\delta)}{4}, \quad (96)$$

$$b_1 = \frac{\sin(2\psi)\cos(\Delta)}{2} + \frac{\sin(2\psi)\cos(\Delta)\cos(\delta)}{2} + \sin(2\psi)\sin(\Delta)\sin(\delta), \quad (97)$$

$$b_2 = \frac{\sin(2\psi)\cos(\Delta)}{2} + \frac{\sin(2\psi)\sin(\Delta)\sin(\delta)}{2}, \quad (98)$$

$$b_3 = \frac{\sin(2\psi)\cos(\Delta)}{2} - \frac{\sin(2\psi)\cos(\Delta)\cos(\delta)}{2}, \quad (99)$$

and

$$b_3 = \frac{\sin(2\psi)\cos(\Delta)}{4} - \frac{\sin(2\psi)\cos(\Delta)\cos(\delta)}{4}. \quad (100)$$

Using Eqs. (93)–(95), we can find ψ and Δ in terms of AC Fourier coefficients a_1 , a_2 , and a_3 ,

$$\sin(\psi) = \sqrt{\frac{a_1 + a_3}{2}}, \quad (101)$$

$$\cos(\psi) = \sqrt{\frac{a_1 + a_3 - 4a_2}{2}}, \quad (102)$$

$$\tan(\psi) = \sqrt{\frac{a_1 + a_3}{a_1 + a_3 - 4a_2}}, \quad (103)$$

and

$$\cos(\Delta) = \frac{b_3}{(1 - \cos(\delta))\sin(\psi)\cos(\psi)}. \quad (104)$$

As mentioned above, $\delta\psi$ and $\delta\cos(\Delta)$ can be obtained by differentiating Eqs. (103) and (104) as

$$\delta\psi = \frac{\delta\psi}{\delta a_1}\delta a_1 + \frac{\delta\psi}{\delta a_2}\delta a_2 + \frac{\delta\psi}{\delta a_3}\delta a_3, \quad (105)$$

$$\delta\cos(\Delta) = \frac{\delta\cos(\Delta)}{\delta a_1}\delta a_1 + \frac{\delta\cos(\Delta)}{\delta a_2}\delta a_2 + \frac{\delta\cos(\Delta)}{\delta a_3}\delta a_3 + \frac{\delta\cos(\Delta)}{\delta b_3}\delta b_3, \quad (106)$$

where

$$\frac{\delta\psi}{\delta a_1} = \frac{1}{1 + \tan^2(\psi)} \frac{1}{4\cos^2(\psi)} (\cot(\psi) - \tan(\psi)), \quad (107)$$

$$\frac{\delta\psi}{\delta a_2} = \frac{1}{1 + \tan^2(\psi)} \frac{1}{4\cos^2(\psi)} (\tan(\psi)), \quad (108)$$

$$\frac{\delta\psi}{\delta a_3} = \frac{1}{1 + \tan^2(\psi)} \frac{1}{4\cos^2(\psi)} (\cot(\psi) - \tan(\psi)), \quad (109)$$

$$\frac{\delta\cos(\Delta)}{\delta a_1} = \frac{-\cos(\Delta)}{4} \left(\frac{1}{\cos^2(\psi)\sin^2(\psi)} \right), \quad (110)$$

$$\frac{\delta\cos(\Delta)}{\delta a_2} = \frac{\cos(\Delta)}{4} \left(\frac{1}{\cos^2(\psi)} \right), \quad (111)$$

$$\frac{\delta\cos(\Delta)}{\delta a_3} = \frac{-\cos(\Delta)}{4} \left(\frac{1}{\cos^2(\psi)\sin^2(\psi)} \right), \quad (112)$$

and

$$\frac{\delta\cos(\Delta)}{\delta b_3} = \frac{1}{(1 - \cos(\delta))\sin(\psi)\cos(\psi)}. \quad (113)$$

5.3. Rotating polarizer compensator ellipsometer with a speed ratio 1:3

Another ellipsometric configuration can be obtained by letting $N_1 = 1$ and $N_2 = 3$ provided that $N_3 = 0$, $\kappa = 0$, $\gamma = 0$, and $\alpha = \pi/4$. We still have a rotating polarizer compensator ellipsometer with a speed ratio 1:3. When these values are inserted into Eq. (24), the Fourier transformation is found to

have twelve AC terms in addition to the DC term, then

$$I(t) = a_0 + \sum_{n=1}^6 a_n \cos(2n\omega t) + \sum_{n=1}^6 b_n \sin(2n\omega t), \quad (114)$$

where

$$a_0 = 1 - \frac{\cos(2\psi)}{4} - \frac{\cos(2\psi)\cos(\delta)}{4}, \quad (115)$$

$$a_1 = 1 - \frac{\cos(2\psi)}{2} - \frac{\cos(2\psi)\cos(\delta)}{2}, \quad (116)$$

$$a_2 = -\frac{\cos(2\psi)}{4} - \frac{\cos(2\psi)\cos(\delta)}{4}, \quad (117)$$

$$a_3 = 0, \quad (118)$$

$$a_4 = -\frac{\cos(2\psi)}{4} + \frac{\cos(2\psi)\cos(\delta)}{4}, \quad (119)$$

$$a_5 = -\frac{\cos(2\psi)}{2} + \frac{\cos(2\psi)\cos(\delta)}{2}, \quad (120)$$

$$a_6 = -\frac{\cos(2\psi)}{4} + \frac{\cos(2\psi)\cos(\delta)}{4}, \quad (121)$$

$$b_1 = \frac{\sin(2\psi)\cos(\Delta)}{2} + \frac{\sin(2\psi)\cos(\Delta)\cos(\delta)}{2} + \frac{\sin(2\psi)\sin(\Delta)\sin(\delta)}{2}, \quad (122)$$

$$b_2 = \frac{\sin(2\psi)\cos(\Delta)}{2} + \frac{\sin(2\psi)\cos(\Delta)\cos(\delta)}{2} - \sin(2\psi)\sin(\Delta)\sin(\delta), \quad (123)$$

$$b_3 = \frac{\sin(2\psi)\sin(\Delta)\sin(\delta)}{2}, \quad (124)$$

$$b_4 = \frac{\sin(2\psi)\cos(\Delta)}{4} - \frac{\sin(2\psi)\cos(\Delta)\cos(\delta)}{4}, \quad (125)$$

$$b_5 = \frac{\sin(2\psi)\cos(\Delta)}{2} - \frac{\sin(2\psi)\cos(\Delta)\cos(\delta)}{2}, \quad (126)$$

and

$$b_6 = \frac{\sin(2\psi)\cos(\Delta)}{4} - \frac{\sin(2\psi)\cos(\Delta)\cos(\delta)}{4}. \quad (127)$$

Solving Eqs. (116), (120), and (126) for ψ and Δ in terms of a_1 , a_5 , and b_5 , we obtain

$$\sin(\psi) = \sqrt{\frac{a_1 + a_5}{4}}, \quad (128)$$

$$\cos(\psi) = \sqrt{\frac{4 - a_1 - a_5}{4}}, \quad (129)$$

$$\tan(\psi) = \sqrt{\frac{a_1 + a_5}{4 - a_1 - a_5}}, \quad (130)$$

$$\cos(\Delta) = \frac{b_5}{(1 - \cos(\delta))\sin(\psi)\cos(\psi)}. \quad (131)$$

$\delta\psi$ and $\delta\cos(\Delta)$ are now given as follows:

$$\delta\psi = \frac{\delta\psi}{\delta a_1}\delta a_1 + \frac{\delta\psi}{\delta a_5}\delta a_5, \quad (132)$$

$$\delta\cos(\Delta) = \frac{\delta\cos(\Delta)}{\delta a_1}\delta a_1 + \frac{\delta\cos(\Delta)}{\delta a_5}\delta a_5 + \frac{\delta\cos(\Delta)}{\delta b_5}\delta b_5, \quad (133)$$

where

$$\frac{\delta\psi}{\delta a_1} = \frac{1}{1 + \tan^2(\psi)} \frac{1}{8\cos^2(\psi)} (\cot(\psi) + \tan(\psi)), \quad (134)$$

$$\frac{\delta\psi}{\delta a_5} = \frac{1}{1 + \tan^2(\psi)} \frac{1}{8 \cos^2(\psi)} (\cot(\psi) + \tan(\psi)), \quad (135)$$

$$\frac{\delta \cos(\Delta)}{\delta a_1} = \frac{[-\tan(\psi) + \cot(\psi)] \cos(\Delta)}{8 \sin(\psi) \cos(\psi)}, \quad (136)$$

$$\frac{\delta \cos(\Delta)}{\delta a_5} = \frac{[-\tan(\psi) + \cot(\psi)] \cos(\Delta)}{8 \sin(\psi) \cos(\psi)}, \quad (137)$$

and

$$\frac{\delta \cos(\Delta)}{\delta b_5} = \frac{1}{(1 - \cos(\delta)) \sin(\psi) \cos(\psi)}. \quad (138)$$

6. Results and discussion

We have discussed two cases: rotating compensator analyzer with fixed polarizer ellipsometer (RCAE) and rotating polarizer and compensator with fixed analyzer ellipsometer (RPCE). For each case, three different speed ratios for the rotating optical elements are assumed. In this section we present the results obtained when applying these configurations to c-Si and GaAs samples. We assume a sample consisting of one interface to separate a semi-infinite air layer of refractive index n_0 as an ambient and a bulk c-Si material of refractive index n_1 . The incidence angle is taken to be $\theta_0 = 70^\circ$. The most common compensators are usually made from CaCO_3 crystal (calcite), MgF_2 , and mica. CaCO_3 compensators are rarely used because the value of $|n_e - n_o|$ is relatively large. In spectroscopic ellipsometry MgF_2 and mica are commonly used. We here assume MgF_2 compensator to have a retardance of $\pi/2$ at 4 eV. The extraordinary and ordinary refractive indices of the compensator are taken from the Handbook of optical constants of solids.^[27]

Based on Eq. (24), simulated light signals are generated. The Fourier transform of the generated signal is taken to extract the Fourier coefficients using the equations derived above for each ellipsometric configuration. The ellipsometric parameters ψ and Δ in the photon energy range of 1.5 eV–6 eV are then derived using Eqs. (32) and (33) for RCAE with speed ratio 1:1, Eqs. (46) and (47) for RCAE with speed ratio 1:2, Eqs. (63) and (64) for RCAE with speed ratio 1:3, Eqs. (82) and (83) for RPCE with speed ratio 1:1, Eqs. (103) and (104) for RPCE with speed ratio 1:2, and Eqs. (130) and (131) for RPCE with speed ratio 1:3. These values of the ellipsometric parameters correspond to the clean signal without considering any noise. In practical situations, random fluctuations in the recorded signal appear due to the noise from many sources. To simulate reality, a random noise is generated using MathCAD code and was superimposed on the clean signal according to the following equation:

$$I_{\text{noise}} = (\text{rnd}(c) - c/2)I + (\text{rnd}(e) - e/2) + 0.0001I_{\text{max}}, \quad (139)$$

where MathCAD's $\text{rnd}(c)$ function produces random noise in a

range from 0 to c and $\text{rnd}(e)$ function produces random noise in the range from 0 to e . Figure 1 shows the noise superimposed on the clean signal.

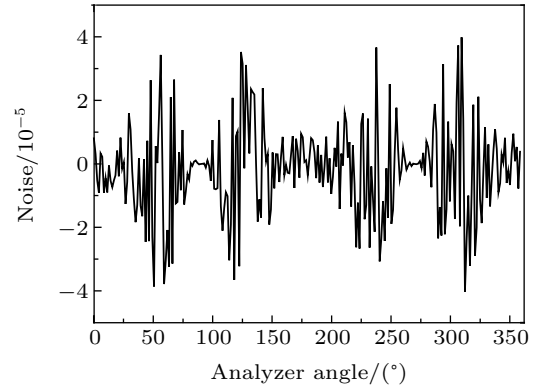


Fig. 1. Noise superimposed on the clean signal.

This noise is added to the pure signal. Fourier transform of the noisy signal is taken to extract the new Fourier coefficients in the presence of the noise. The same equations are then used to calculate the ellipsometric parameters ψ and Δ for the noisy signal in the same photon energy range. To calculate the complex refractive index of the sample, we use Eq. (5).

6.1. n and k of c-Si and GaAs

The calculated values of n and k for c-Si and GaAs are plotted in Figs. 2 and 3, respectively along with the published values.^[27] The points in Figs. 2 and 3 represent the calculated real and imaginary parts of the refractive index of c-Si and GaAs for the noisy signal using RCAE with speed ratio 1:1. If another ellipsometric configuration is used the difference between them cannot be obviously observed in this figure. To differentiate among them, we calculate the percentage error in the calculated values of n and k for each ellipsometric configuration.

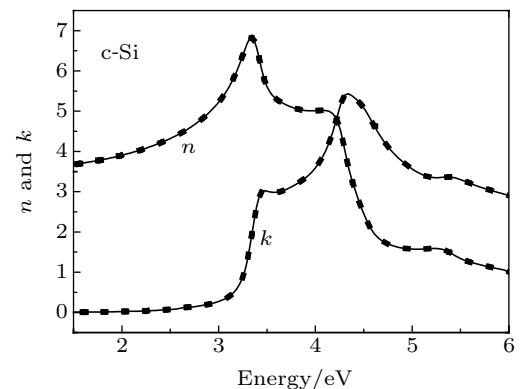


Fig. 2. Real and imaginary parts of the refractive index of c-Si in a photon energy range from 1.5 eV to 6 eV. Lines represent accepted values, and points denote calculated values.

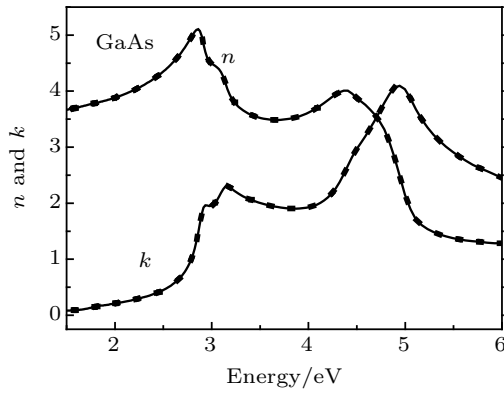


Fig. 3. Real and imaginary parts of the refractive index of GaAs in a photon energy range from 1.5 eV to 6 eV. Lines represent accepted values, and points denote calculated values.

6.2. Percentage error in n and k of c-Si and GaAs

The percentage errors in the calculated values of n have been calculated for the two samples (c-Si, GaAs) as shown in Figs. 4 and 5 for all ellipsometric configurations which are rotating polarizer and compensator with fixed analyzer (RPCE) using different speed ratios as well as rotating compensator and analyzer with fixed polarizer (RCAE) using different speed ratios. We should emphasize that the fluctuations shown in the two figures are due to the noise imposed on the clean signal as mentioned before. Generally, the percentage errors in n for the two samples are low (of order 10^{-2}) for all ellipsometric configurations. As a result, the comparison of percentage error in n among them is not of high significance.

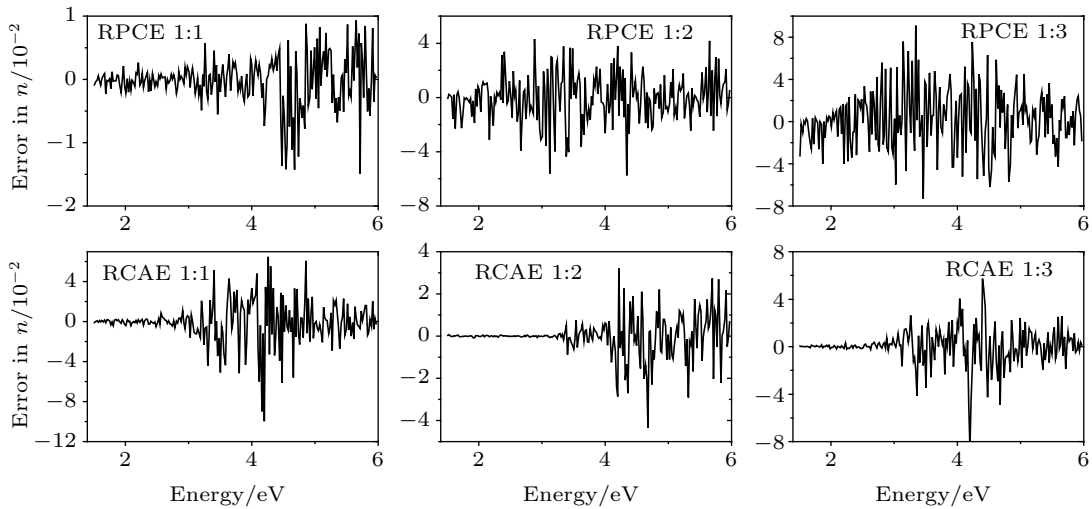


Fig. 4. Percentage errors in the real part of the refractive index of c-Si for all the ellipsometric configurations.

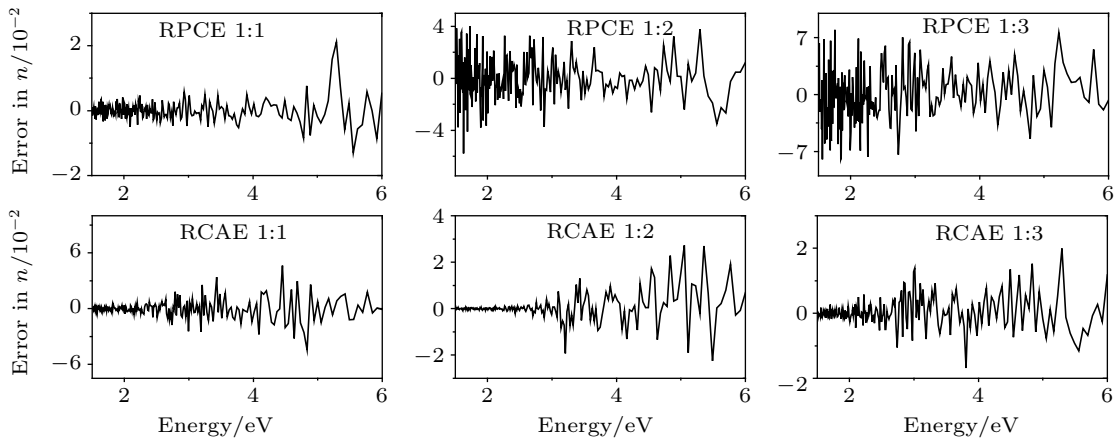


Fig. 5. Percentage errors in the real part of the refractive index of GaAs for all the ellipsometric configurations.

Figures 6 and 7 show the percentage errors in k for the two samples. As can be seen from the figures, the percentage error in k is much higher than that in n . Moreover, this percentage error in k is crucially dependent on the ellipsometric configuration used. The two figures show that the RCAE with speed ratio 1:2 corresponds to the minimum percentage error in k . For c-Si sample, the percentage error ranges from -0.1% to 0.08% as shown in Fig. 6 whereas it ranges between $\pm 0.02\%$

for GaAs sample as shown in Fig. 7. We can conclude that the RCAE with speed ratio 1:2 has a preference among other configurations. It is worth mentioning that these values of n and k were calculated using a set of AC Fourier coefficients without dependence on the DC coefficient. If the DC term is considered in the calculations, the percentage errors in n and k would be much higher.^[19,23]

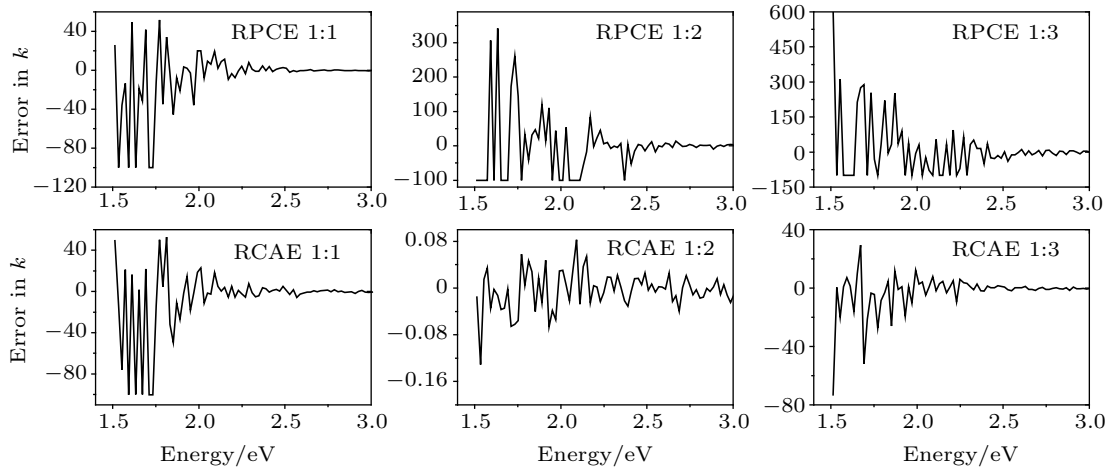


Fig. 6. Percentage errors in the imaginary part of the refractive index of GaAs for all the ellipsometric configurations.

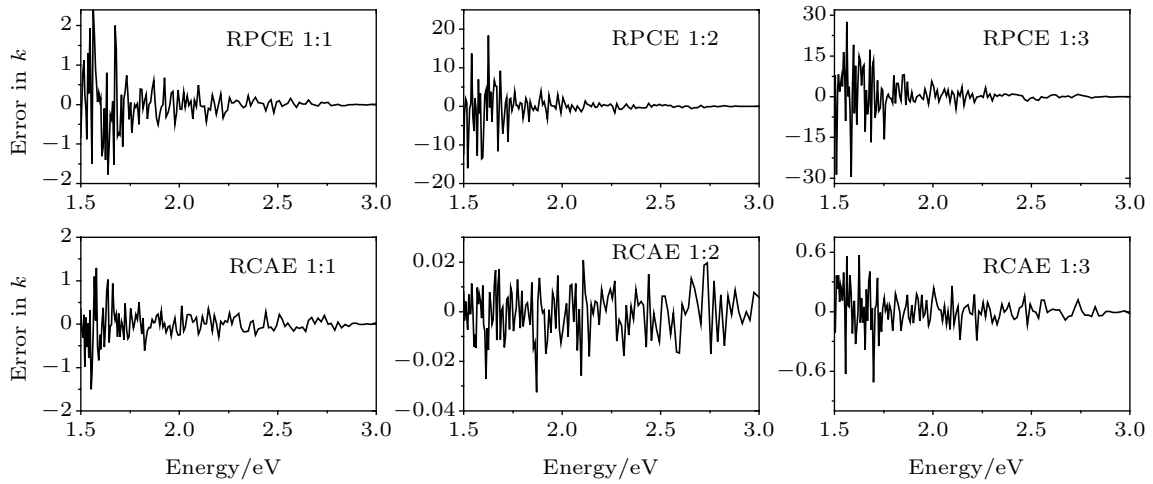


Fig. 7. Percentage errors in the imaginary part of the refractive index of GaAs in a photon range from 1.5 eV to 3 eV for all the ellipsometric configurations.

6.3. Uncertainties

In this subsection, we investigate the uncertainties $\delta \cos(\Delta)$ and $\delta \psi$ in ψ and $\cos(\Delta)$ as functions of the uncertainties of the Fourier coefficients. $\delta \cos(\Delta)$ and $\delta \psi$ represent the fluctuations of $\cos(\Delta)$ and ψ about their ideal values respectively. The uncertainties $\delta \cos(\Delta)$ and $\delta \psi$ for c-Si sample for the six configurations are plotted in Figs. 8–11. Figure 8 shows the curves of $\delta \cos(\Delta)$ versus energy for the RCAE with speed ratios 1:1, 1:2, and 1:3. The first three panels in the figure show the curves of $\delta \cos(\Delta)$ versus energy due to the uncertainty of the Fourier coefficients for each ellipsometric configuration. For example, the first panel (upper left) shows $\delta \cos(\Delta)$ due to the uncertainty of a_1 and a_3 using the RCAE with a speed ratio 1:1. The fourth panel (lower right) shows the total variation in $\cos(\Delta)$ due to simultaneous uncertainty in all Fourier coefficients. From the figure we see that the structure that has the lowest uncertainty is for the case of 1:2 and this is in agreement with the conclusion mentioned in the previous subsection. In a similar manner, Fig. 9 shows the un-

certainty in $\cos(\Delta)$ of the RPCE with speed ratios 1:1, 1:2, and 1:3. Comparing the two figures (Figs. 8 and 9), we can conclude that the RCAE with the speed ratio 1:2 is still the best structure due to the minimum percentage error obtained with this configuration.

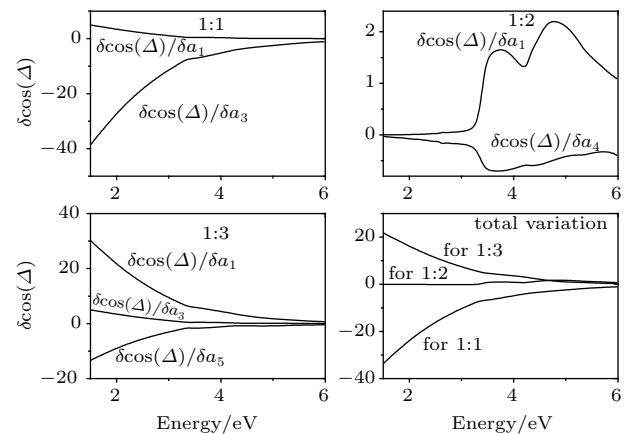


Fig. 8. Curves of $\delta \cos(\Delta)$ versus energy in different RCAE structures.

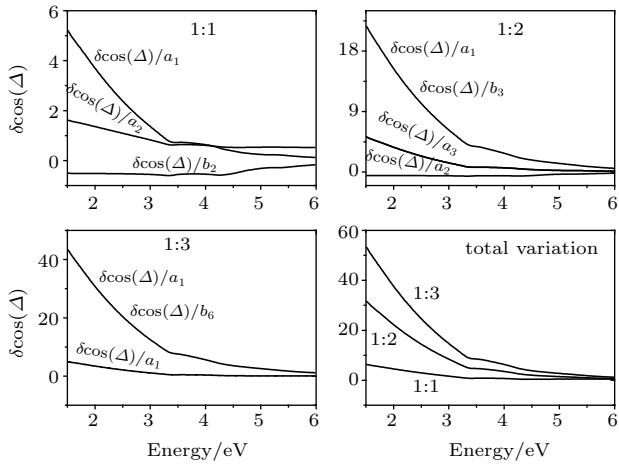


Fig. 9. Curves of $\delta \cos(\Delta)$ versus energy in different RPCE structures.

The uncertainties in ψ for the RPCE with different speed ratios are shown in Fig. 10 whereas they are shown in Fig. 11 for RCAE. As can be seen from the two figures, the ellipsometric parameter ψ is less sensitive to the uncertainty in the Fourier coefficients than Δ . Moreover, the sensitivity of ψ to the uncertainty in the Fourier coefficients is high in the low energy region compared with in the low energy region for all ellipsometric configurations. Figure 11 reveals that the RCAE with the speed ratio 1:2 is still the best structure due to the low sensitivity of this configuration in all configurations.

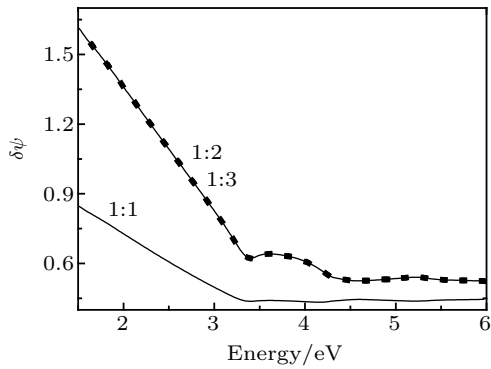


Fig. 10. Curves of $\delta \psi$ versus energy in RPCE structures with speed ratios 1:1, 1:2, and 1:3.

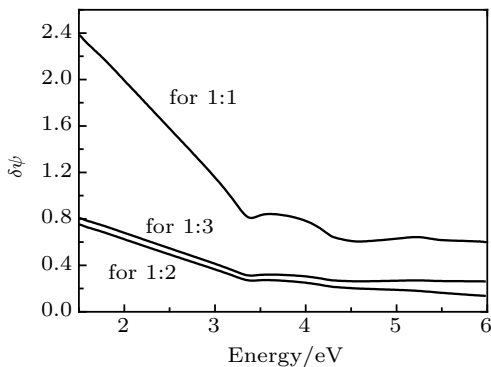


Fig. 11. Curves of $\delta \psi$ versus energy in RCAE structures with speed ratios 1:1, 1:2, and 1:3.

6.4. Misalignment of the optical elements

In practical situations, the alignment of the optical elements with respect to the plane of incidence is not easy. Azimuthal misalignment of optical elements is considered as one of the most affecting sources of systematic errors. It is very important to mention systematic error sources in such a structure. Sample mispositioning, beam deviation, collimation errors, and azimuthal misalignment of optical elements are the usual sources of systematic errors. Thus, it is important for the verification process to have some quantities for the determination of the accuracy of the simulated data as a result of misalignment of the polarizer and rotating compensator. The parameters to be checked are the ellipsometric parameters ψ and Δ as well as the real and imaginary parts of refractive indices n and k .

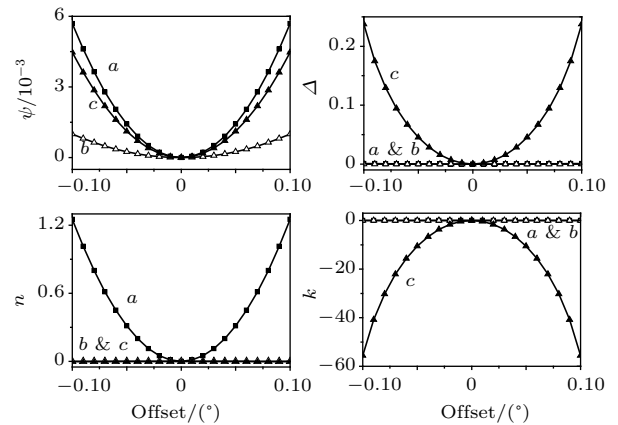


Fig. 12. Percentage errors in n , k , ψ , and Δ for c-Si sample at $\lambda = 632.8$ nm each as a function of the error in γ while keeping the two other variables (κ and α) equal to zero. The figure represents RCAE with speed ratios: curve a 1:1, curve b 1:2, and curve c 1:3 (RCAE offset in γ).

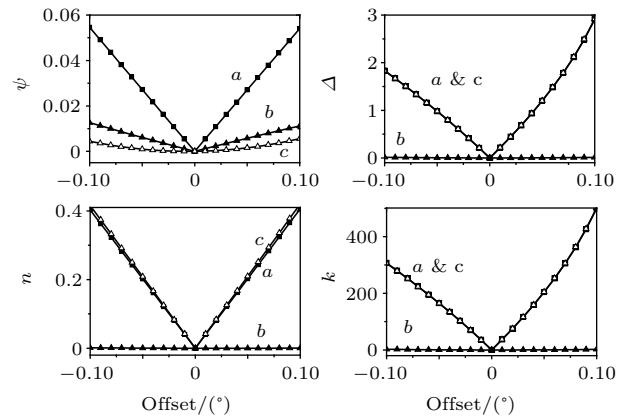


Fig. 13. Percentage errors in n , k , ψ , and Δ for c-Si sample at $\lambda = 632.8$ nm each as a function of the error in γ while keeping the two other variables (κ and α) equal to zero. The figure represents RPCE with speed ratios: curve a 1:1, curve b 1:2, and curve c 1:3 (RPCE offset in γ).

Figures 12 and 13 show the percentage errors in ψ , Δ , n , and k for RCAE and RPCE respectively each as a function of the error in the polarizer azimuth angle γ varying from -0.1° to 0.1° in steps of 0.01° while keeping the other variables equal to zero. Each figure shows the three ellipsometric

configurations with the speed ratios 1:1, 1:2, and 1:3. As can be seen from the figures, the influence of misalignment of the rotating polarizer on ψ , Δ , and n is not significant for small misalignment. On the other hand, it is considerable for k especially for RPCE with the speed ratio 1:3.

Similarly, Figs. 14 and 15 show the errors in the same parameters for RPCE and RCAE for three speed ratios each as a function of the error in the rotating compensator azimuth angle κ varying from -0.1° to 0.1° in steps of 0.01° while keeping the other variables equal to zero. Almost the same conclusions drawn from Figs. 12 and 13 can describe Figs. 14 and 15. The influence of misalignment of the rotating compensator on ψ , Δ , and n is not considerable whereas it is relatively high for k , especially for RPCE with the speed ratio 1:3.

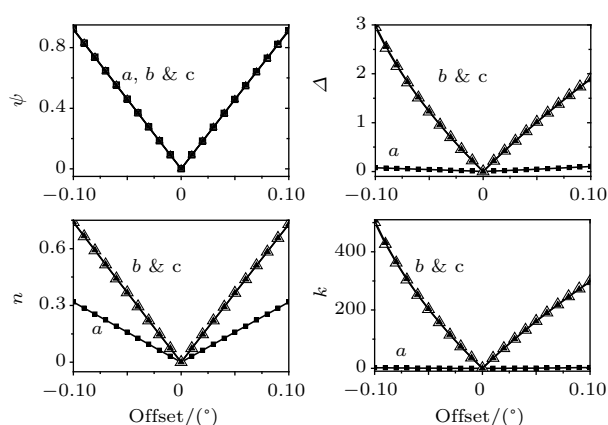


Fig. 14. Percentage errors in n , k , ψ , and Δ for c-Si sample at $\lambda = 632.8$ nm each as a function of the error in κ while keeping the two other variables (γ and α) equal to zero. The figure represents RPCE with speed ratios: curve a 1:1, curve b 1:2, and curve c 1:3 (RPCE offset in k).

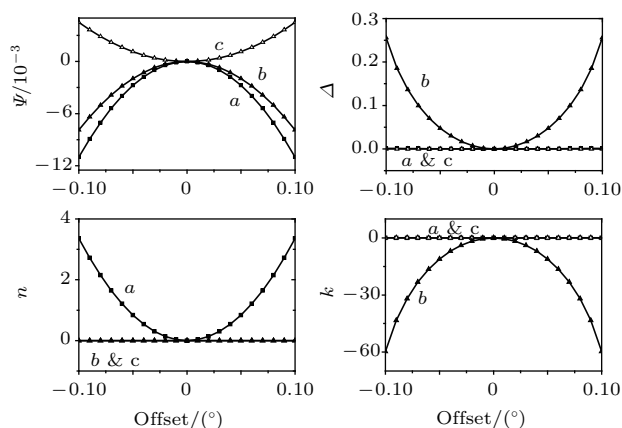


Fig. 15. Percentage errors in n , k , ψ , and Δ for c-Si sample at $\lambda = 632.8$ nm each as a function of the error in κ while keeping the two other variables (γ and α) equal to zero. The figure represents RCAE with speed ratios: curve a 1:1, curve b 1:2, and curve c 1:3 (RCAE offset in k).

Finally, it is worth comparing the best configuration which is RCAE at a speed ratio 1:2 with the well-known rotating compensator ellipsometer RCE.^[28] Figure 16 shows the total variation of $\cos(\Delta)$ due to simultaneous uncertainty in all

Fourier coefficients for RCE and RCAE at a speed ratio 1:2. The sensitivity of $\cos(\Delta)$ in the case of RCAE is much less than that in case of RCE especially for photon energies less than 3 eV. Therefore the preference of RCAE at a speed ratio 1:2 over the RCE is clear in the figure.

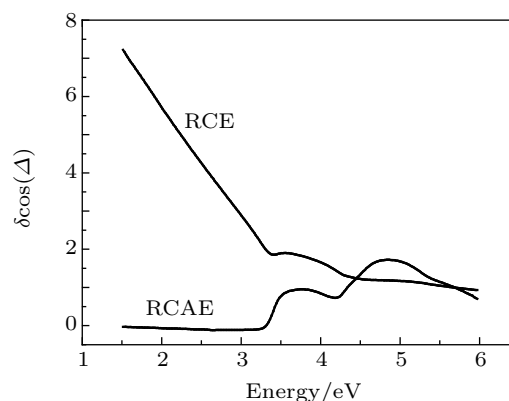


Fig. 16. Curves of $\delta \cos(\Delta)$ versus energy for RCE and RCAE at a speed ratio 1:2.

7. Conclusions

We present two ellipsometric structures, which are rotating polarizer compensator (RPCE) and rotating compensator analyzer (RCAE). For each structure, we assume three different configurations by considering different speed ratios. The percentage errors arising from noise effects and misalignment of the optical elements are investigated for all configurations. Moreover, the uncertainty in the ellipsometric parameters due to the uncertainty in Fourier coefficients is presented. We find that RCAE with a speed ratio 1:2 corresponds to the smallest error in the calculated optical parameters of two samples. A comparison between the well-known rotating compensator ellipsometry (RCE) and RCAE at a speed ratio 1:2 reveals that RCAE has a preference over RCE.

References

- [1] Li S 2000 *J. Opt. Soc. Am. A* **17** 920
- [2] El-Agez T and Taya S A 2011 *Opt. Lasers Eng.* **49** 507
- [3] Smith M H 2002 *Appl. Opt.* **41** 2488
- [4] Taya S A and El-Agez T 2011 *Optik* **122** 666
- [5] Smith M H 2002 *Appl. Opt.* **41** 2488
- [6] Taya S A and El-Agez T 2011 *Turkish J. Phys.* **35** 31
- [7] Martino A D, Garcia-Caurel B, Laude B and Drevillon B 2004 *Thin Solid Films* **455** 112
- [8] El-Agez T, Tayyan A A, Taya S A and Musleh H S 2011 *The Islamic University Journal* (Series of Natural Studies and Engineering) **19** 163
- [9] Broch L and Johann L 2008 *Phys. Status Solidi* **5** 1036
- [10] El-Agez T M, Wieliczka D M, Moffitt C and Taya S A 2011 *Phys. Scr.* **84** 045302 doi:10.1088/0031-8949/84/04/045302
- [11] El-Agez T M, Wieliczka D M, Moffitt C and Taya S A 2011 *J. At. Mol. Opt. Phys.* **2011** 295304 doi:10.1155/2011/295304
- [12] Azzam R M and Bashara N M 1977 *Ellipsometry and Polarized Light* (Amsterdam: North-Holland)

- [13] Fujiwara H 2007 *Spectroscopic Ellipsometry Principles and Applications* (West Sussex: John Wiley & Sons)
- [14] Aspnes D E and Studna A A 1975 *Appl. Opt.* **14** 220
- [15] Muller R H and Farmer J C 1984 *Rev. Sci. Instrum.* **55** 371
- [16] Aspnes D E 1973 *Opt. Commun.* **8** 222
- [17] El-Agez T M and Taya S A 2011 *Phys. Scr.* **83** 025701
- [18] Chen LY, Feng X W, Su Y, Ma H Z and Qian Y H 1994 *Appl. Opt.* **33** 1299
- [19] El-Agez T M and Taya S A 2010 *J. Sensors* **2010** 706829 doi:10.1155/2010/706829
- [20] El-Agez T and Taya S A 2011 *Int. J. Microwave Opt. Technol. (IJMOT)* **6** 363
- [21] El-Agez T, Taya S A and El Tayayn A 2011 *Int. J. Optomechatronics* **5** 51
- [22] Taya S A, El-Agez T M and AlKanoo A A 2011 *J. Electromag. Anal. Appl.* **3** 351
- [23] El-Agez T M, El Tayyan A A and Taya S A 2010 *Thin Solid Films* **518** 5610
- [24] Taya S A, El-Agez T M and AlKanoo A A 2012 *Chin. Phys. B* **21** 110701
- [25] Zhang Q X, Wei W S and Ruan F P 2011 *Chin. Phys. B* **20** 047802
- [26] Zhang J T, Wu X J and Li Y 2012 *Chin. Phys. B* **21** 010701
- [27] Palik E D 1985 *Handbook of Optical Constants of Solids* (San Diego: Academic Press, CA)
- [28] Aspnes D E 2004 *J. Opt. Soc. Am. A* **21** 403